Since January 2020 Elsevier has created a COVID-19 resource centre with free information in English and Mandarin on the novel coronavirus COVID-19. The COVID-19 resource centre is hosted on Elsevier Connect, the company's public news and information website.

Elsevier hereby grants permission to make all its COVID-19-related research that is available on the COVID-19 resource centre - including this research content - immediately available in PubMed Central and other publicly funded repositories, such as the WHO COVID database with rights for unrestricted research re-use and analyses in any form or by any means with acknowledgement of the original source. These permissions are granted for free by Elsevier for as long as the COVID-19 resource centre remains active.

Biomedicine & Pharmacotherapy 152 (2022) 113223

Contents lists available at ScienceDirect

Biomedicine & Pharmacotherapy

journal homepage: www.elsevier.com/locate/biopha

Treatment with metformin glycinate reduces SARS-CoV-2 viral load: An *in vitro* model and randomized, double-blind, Phase IIb clinical trial

Claudia Ventura-López [a,1], Karla Cervantes-Luevano [a,1], Janet S. Aguirre-Sánchez [b], Juan C. Flores-Caballero [b], Carolina Alvarez-Delgado [a], Johanna Bernaldez-Sarabia [a], Noemí Sánchez-Campos [a], Laura A. Lugo-Sánchez [c], Ileana C. Rodríguez-Vázquez [c], Jose G. Sander-Padilla [c], Yulia Romero-Antonio [c], María M. Arguedas-Núñez [c], Jorge González-Canudas [c], Alexei F. Licea-Navarro [a,*]

[a] *Departamento de Innovación Biomédica, CICESE, Carretera Ensenada-Tijuana 3918, Zona Playitas, Ensenada, BC 22860, Mexico*
[b] *The American British Cowdray Medical Center I.A.P. (Centro Médico ABC), Mexico*
[c] *Laboratorio Silanes S.A. de C.V., CdMx, Mexico*

ARTICLE INFO

Keywords:
SARS-CoV-2 viral load
COVID-19 treatment
Metformin glycinate
SARS-CoV-2 variants

ABSTRACT

The health crisis caused by the new coronavirus SARS-CoV-2 highlights the need to identify new treatment strategies for this viral infection. During the past year, over 400 coronavirus disease (COVID-19) treatment patents have been registered; nevertheless, the presence of new virus variants has triggered more severe disease presentations and reduced treatment effectiveness, highlighting the need for new treatment options for the COVID-19. This study evaluates the Metformin Glycinate (MG) effect on the SARS-CoV-2 *in vitro* and *in vivo* viral load. The *in vitro* study was conducted in a model of Vero E6 cells, while the *in vivo* study was an adaptive, two-armed, randomized, prospective, longitudinal, double-blind, multicentric, and phase IIb clinical trial. Our *in vitro* results revealed that MG effectively inhibits viral replication after 48 h of exposure to the drug, with no cytotoxic effect in doses up to 100 μM. The effect of the MG was also tested against three variants of interest (alpha, delta, and epsilon), showing increased survival rates in cells treated with MG. These results are aligned with our clinical data, which indicates that MG treatment reduces SARS-CoV2-infected patients' viral load in just 3.3 days and supplementary oxygen requirements compared with the control group. We expect our results can guide efforts to position MG as a therapeutic option for COVID-19 patients.

1. Introduction

A novel coronavirus was recently discovered and termed SARS-CoV-2. Human infection can cause coronavirus disease 2019 (COVID-19), for which, at this point, over 510 million cases have resulted in more than 6 million deaths in over 40 countries; in Mexico, there are over 5 million cases with more than 300,000 deaths [1]. SARS-CoV-2 infects different organs and causes a systemic disease; as clearance of the virus occurs, the symptoms tend to worsen, implicating an aberrant immune response as pathogenesis of infection [2]. COVID-19 has presented one of the most significant challenges to humanity concerning the development of diagnostic systems, vaccines, and new treatments. A detailed search in the Orbit database indicated that between January 2020 to August 2021, 439 relevant patents and applications were registered relating to the treatment of the infection caused by the coronavirus SARS-CoV-2, including compounds of traditional Chinese medicine, as well as a wide variety of treatments comprising placenta-derived natural killer cells, ILC3 cells derived from a population of hematopoietic stem or

* Corresponding author.
E-mail addresses: cventura@cicese.mx (C. Ventura-López), kcervates@cicese.mx (K. Cervantes-Luevano), janetaguirre@yahoo.com (J.S. Aguirre-Sánchez), juancarlosfl18@hotmail.com (J.C. Flores-Caballero), alvarezc@cicese.mx (C. Alvarez-Delgado), jbernald@cicese.mx (J. Bernaldez-Sarabia), lsanchez@cicese.mx (N. Sánchez-Campos), llugo@silanes.com.mx (L.A. Lugo-Sánchez), icrodriguez@silanes.com.mx (I.C. Rodríguez-Vázquez), jgsander@silanes.com.mx (J.G. Sander-Padilla), yromero@silanes.com.mx (Y. Romero-Antonio), marguedas@silanes.com.mx (M.M. Arguedas-Núñez), jogonzalez@silanes.com.mx (J. González-Canudas), alicea@cicese.mx (A.F. Licea-Navarro).
[1] These authors contribute equally to this work.

https://doi.org/10.1016/j.biopha.2022.113223
Received 20 March 2022; Received in revised form 25 May 2022; Accepted 30 May 2022
Available online 2 June 2022
0753-3322/© 2022 The Authors. Published by Elsevier Masson SAS. This is an open access article under the CC BY license (http://creativecommons.org/licenses/by/4.0/).

progenitor cells, antibodies, an alpaca nanobody, modified viruses, bacteria (*Pseudomonas*), recombinant plasmids, oligomannuronic acid phosphate, chitosan, ketoamide-based compounds, extracellular polysaccharide metabolite of yeast, "halogen or halogenated" compounds for inhibiting ion channel activity of SARS-CoV-2E protein, thioimidazolidinone to dysregulate Angiotensin-converting enzyme (ACE) and TMPRSS2 (Spike) proteins, GP73 inhibitor to reduce the enrichment of ACE2 in the cell membrane preventing the virus infection, xanthine oxidase inhibitor and an active oxygen scavenger that modifies disulfide bonds in viral receptors, altering the affinity between the viral receptor and the spike protein (S), inhibiting the virus proliferation, membrane fusion inhibitor polypeptide, viral replication inhibitors, pinocytosis inhibitors of the virus in host cells, activity inhibitor of virus protease 3CL pro and viral RNA-dependent RNA polymerase (RdRp) inhibitor. Treatments involving drug repositioning also stand out, such as Remdesivir, Ivermectin, and their respective modifications. However, the presence of mutations or substitutions in amino acids of the S protein give place to new virus variants with implications for public health such, as an increase in transmissibility, more severe disease presentations, and reduced effectiveness of treatments or vaccines; highlighting the need to identify new treatment strategies for these viral infections.

Metformin (Met) is a biguanide widely used to treat type 2 diabetes [3], a disease that increases the risk of mortality in patients with COVID-19 infection. Recently, metformin glycinate (MG), a new drug derived from Met, has been shown to have better bioavailability, absorption, and safety profile than Met, with comparable antihyperglycemic effects [4,5]. Met and MG have different mechanisms of action: Met has been shown to selectively inhibit mitochondrial complex I (NADH dehydrogenase), leading to less oxygen consumption rate, lower ATP levels, and the activation of AMP-activated protein kinase (AMPK) [6].

On the other hand, four lines of work characterize the mechanism of action of MG. They are a function of different proteins: Goodpasture antigen-binding Protein (GPBP), Liver Kinase B1 (LKB1), AMPK, and Akt substrate of 160 kDa (AS160), which are essential in regulating the activity of the ceramide transporter (CERT), energy, and glucose metabolism [6,7]. So far, based on the evidence [8–14] it has been determined that: it inhibits kinase activity GPBP/CERT activity. GPBP/CERT and LKB1 synergistically enhance their kinase activity, AMPK increases GPBP/CERT activity, increases the activity of LKB1 (metformin does not), and inhibits the cross-activation of GPBP/CERT and LKB1. Provides a different profile modulation of the immune response, especially with the migration of M1 to M2 by inhibiting the synthesis of Interleukin 10 (IL10), translocate the Glucose transporter (GLUT4) more efficiently, consequently acts *via* the VAPA-VAMP2 interaction, and participates in the regulation of AS160. Metformin glycinate is the only commercially available inhibitor of kinase activity CERT with safety and efficacy studies.

In this study, we established a human cell culture model for infection of lung cells H1299 with SARS-CoV-2 clinically isolated. Employing this system, we determined the SARS-CoV-2 viral load at different times after infection. In the context of our drug repositioning hypothesis, we tested the capacity of MG to inhibit infection by SARS-CoV-2 in an *in vitro* model of Vero E6 cells. Furthermore, we studied the efficacy and safety of MG for the treatment of hospitalized patients with acute severe respiratory syndrome secondary to SARS-CoV-2, in a randomized, double-blind, phase IIb clinical trial. The fact that MG reduces the protein secretion pathway led us to hypothesize it could also inhibit the secretion of viral particles from infected cells and thus be a candidate for drug repositioning against SARS-CoV-2.

2. Materials and methods

2.1. Viral isolation and cell culture

Cell line H1299 (carcinoma; non-small cell lung cancer) and Vero E6 cell line were obtained from ATCC. Cells were maintained in a Dulbecco's Modified Eagles Medium (DMEM) medium (Corning) containing 10 % of fetal bovine serum (FBS) (Biowest), and 1 % antibiotic/antimycotic (Gibco, 10,000 units/mL of penicillin, 10,000 μg/mL of streptomycin, and 25 μg/mL of Fungizone).

Nasopharyngeal swabs were obtained from patients and identified as positive for SARS-CoV2 infection after RNA extraction with QIAamp Viral RNA Mini Kit (Qiagen) and positive amplification of RNA-dependent RNA polymerase (RdRP) gene by qPCR using qPCRBIO probe 1 step Go No-ROX (PCR biosystems). For viral isolation, the Vero E6 cell line was used at confluency in a T25 cm^2 flask in a modified protocol [15]. Briefly: complete media was removed, and the monolayer was washed twice with phosphate buffer solution (PBS), trypsinized and counted; for infection, a total of 3×10^6 cells were seeded in DMEM 2 % FBS + 1 % antibiotic/antimycotic (infection media) for each nasopharyngeal swab, a control of mocked cell was seeded in parallel. After 24 h, cells reached 80 % confluence and the monolayer was infected with 50 μL of the nasopharyngeal swab in 800 μL of infection media, flask were incubated at 37 °C and 5 % CO_2 and manually moved every 20 min for 2 h; after incubation supernatant was removed and 5 mL of new infection media were added. Cultures were monitored every 24 h for cytopathic effects (CPE). Isolated supernatant was used for sequencing and further experiments; Tissue Culture Infectious Dose 50 % ($TCID_{50}$) and Multiplicity of Infection (MOI) were calculated in Vero E6 cells [16–18]. SARS-CoV2 variants were identified by whole-genome sequencing using Illumina COVIDSeq Assay (Illumina), from viral amplifications of nasopharyngeal swabs with low Cq value; complete viral sequences were assembled and characterized using the Illumina® DRAGEN COVID Lineage App version 3.5.4 (Illumina) and submitted to GISAID.

2.2. In vitro effect of metformin glycinate

For viral load assays in H1299 cells, a total of 5×10^4 cells/well were seeded 24 h before infection with SARS-CoV-2 MX/BC1/2020 at a MOI of 100:1 particle per cell for 2 h in DMEM 2 %FBS + 1 % antibiotic/antimycotic (infection media). After incubation, the supernatant with the inoculum was removed and 500 μL of new infection media was added containing 0, 0.1, 1 or 10 μM of MG. At 24 and 48 h after the drug's addition, the cell supernatant was collected and centrifuged for 5 min at 300 g to remove debris and stored at − 80 °C. Cell monolayers were collected by scraping and resuspending in 500 μL of infection media.

2.2.1. Dose effect of MG on SARS-CoV-2 viral load and cell survival

Both cell monolayers and supernatant were used to isolate RNA using the QIAamp Viral RNA Mini Kit (Qiagen). The obtained RNA was used as a template in the reverse transcription and amplification of the SARS-CoV-2 E gene [19]. For this amplification, the qPCRBIO probe 1 step Go No-ROX (PCR biosystems) kit was used in a final volume of 20 μL contained 1X reaction buffer, 0.4 μM of the forward (5′-ACAGGTACGTTAATAGTTAATAGCGT-3′) and reverse (5′-ATATTGCAGCAGTACGCACACA-3′) primers, 0.2 μM Probe (5′-FAM-ACACTAGCCATCCTTACTGCGCTTCG-BHQ1-3′), 0.2 × of RTase Go, and 5 μL of RNA. Amplification conditions were, Retro-transcription at 50 °C for 15 min, denaturation at 95 °C for 2 min, followed by 45 cycles for 15 s at 95 °C, 30 s at 60 °C acquiring the fluorescence at this step. The RT-qPCR reactions were conducted in duplicate for all samples using a 96-well and optical adhesive film (Bio-Rad, CA, USA) on a CFX96 Real-Time PCR Detection System (Bio-Rad). The determination of the copy numbers was obtained by extrapolation of Cq values in the linear regression curve. The standard curve was obtained from 5 serial dilutions (dilution factor 1:10) of a Synthetic RNA transcribed *in vitro*, ranging from 10^6 to 10^2 molecules SARS-CoV-2 per μL. The synthesized RNA corresponds to a 1000 bp sequence with the SARS-CoV-2 RdRP and E genes inserted. For the statistical analysis, a factorial ANOVA was used to establish differences

between drug concentration, and significance was established at $P < 0.05$.

To evaluate cell death due to the active principle, toxicity controls were set up in parallel with the infection experiments without infection. In short, 0.1, 1.0,10 and 100 μM of MG were added to 5×10^4 H1299 cells/well in cell culture conditions using 10 % DMSO as a dead control, and PBS as a negative control. The final viability of cells after 48 h of exposure was measured in a parallel experiment by a colorimetric method [20,21] using the CellTiter 96® AQueous One Solution Cell Proliferation Assay (Promega). Half-maximal inhibitory concentration (IC50) values were fitting using a dose-response curve in GraphPad prism 9.

2.2.2. Inhibition of SARS-CoV-2 variants cytopathic effects by MG

A total of 1.5×10^4 Vero E6 cells/well were seeded in a 96 well plate for 24 h in infection media as pre-conditioning. After this time, media was removed and cells were pre-incubated with 300 μM of MG for 1 h prior to virus infection with 0.01 pfu/cell of isolated viral strains B.1.387 (D614G); B.1.429 + B.1.427 (Epsilon); B.1.1.7 (alpha) or B.1.617.2 (delta). After 96 h incubation, cytopathic effect on cells was measured by neutral red uptake assay and viral mediated cell death was compared among variants. The nucleoside GS-441524 were used as a positive control for inhibition of viral replication in the same conditions. Differences between the media was evaluated by unpaired student t-test with $p < 0.0001$ with the software GraphPad prism 9.

2.3. Clinical study

An adaptive, two-armed, randomized, prospective, longitudinal, double-blind, multicentric and phase IIb clinical trial was performed, with the main objective of evaluating the efficacy and safety of MG treatment *vs* placebo (Treatment A: Metformin Glycinate 620 mg, administered orally, twice a day for 14 days, Treatment B: Placebo, administered orally, twice a day for 14 days) in patients with severe acute respiratory syndrome secondary to SARS-CoV-2 infection and diagnosis of type 2 diabetes mellitus. The study was conducted from July 2020 to March 2021, with a follow-up period of 14 days. The evaluation criteria were: a) Comparing the viral load between groups; b) analyzing the viral load in the same group at days 0 (basal), 2, 5, 7, 9, and at the end of the study; c) comparing the use of supplementary oxygen, artificial mechanical ventilation, duration of hospital stay, normalization of body temperature, oxygen saturation, and number of deaths, between groups; d) evaluating the change in basal and final levels of serum creatinine, aspartate aminotransferase, and creatine kinase MB (CK-MB); e) and prevalence of grades 3 and 4 adverse events at the beginning and end of the study.

2.3.1. Study subjects

Twenty patients, over 18 years of age, both genders with coronavirus infection, severe acute respiratory syndrome (SARS-CoV)-2 confirmed by polymerase chain reaction (PCR) test ≤ 4 days before randomization, hospitalized and with radiographic evidence of pulmonary infiltrates, were recruited. Patients with multiorgan failure, with mechanical ventilation during the randomization and pregnant women were excluded from the study. Patients were randomly and blindly distributed into "group A" (treatment group that received 620 mg of MG, twice a day) and "group B" (placebo), with 10 patients in each group. All patients signed their informed consent form. This study was conducted in the American British Cowdray Medical Center and was accepted by the Ethical Research Committee of the institution: with approval number ABC-20-16. The study was registered in the Clinical Trials System (NCT04625985) in October 2020, during the enrollment of participants, as well as in the Clinical Trials National Registry (RNEC by its Spanish acronym) with the number 203301410A0085 registered on June 30 of 2020.

2.3.2. Randomization and blinding

Randomization of the treatment group was performed by the principal investigator using a randomization list generated by randomizer.org. Allocation was done by simple random sampling, balanced by treatment. During the enrollment and randomization, no participants were excluded, all 20 participants were randomized and started the study treatments. The blinding of the study was carried out by homologating the tablets and the packaging. The packages were identified by kit number, both the patient and the principal investigator were unaware of the allocation of participants. Breaking of blinding of the study was not required.

2.3.3. Statistical analysis

The efficacy of the treatment was statistically analyzed in "all treated patients" (ATP), a group of all the randomized patients that received at least one dose of MG, and that had a basal and subsequent reading. Missing data were managed using the "last observation carried forward" method. The comparison between the groups of viral load, oxygen supplementation and days of hospital stay was carried out using Student's t-tests for independent samples. The comparison between the groups of the laboratory variables was carried out using the non-parametric Mann Whitney U test. Qualitative variables were analyzed using Fisher's exact-tests. All tests were performed with IBM SPSS Statistics for Windows, version 25 (IBM Corp., Armonk, N.Y., USA). Values of $p < 0.05$ were considered significant.

The sample size was selected to evaluate the primary efficacy in 10 patients infected by SARS-CoV2 *vs* 10 patients with personalized treatment for COVID-19 according to the criteria of the treating physician. Using an adaptive model.

3. Results

3.1. In vitro effect of metformin glycinate

3.1.1. Dose effect and IC50

To test the antiviral effect, three doses of MG 0.1, 1, and 10 μM were added to H1299 cells for 24 and 48 h. Quantification of the extracellular viral load was performed in at least 6 independent replicates. At 24 h after exposition to the drug, no significant differences were observed neither in the cell culture nor in the supernatant (data not shown). As shown in Fig. 1, the major inhibition effect for the presence of virus in the supernatant and cell-associated virus was observed at 48 h. MG shows at 48 h, a 98 % decrease in the viral load in the cell-associated virus (Fig. 1A); and a 86 % decrease of the viral load in the supernatant medium (Fig. 1B). The IC50 value to decrease the cell-associated virus load was 189.8 μM of MG (Fig. 1C), and the IC50 value to decrease the supernatant viral load was 355.4 μM of MG (Fig. 1D).

3.1.2. MG inhibits cytopathic effects mediated by SARS-CoV2 variants

After 48 h of exposure, the drug MG potently inhibits SARS-CoV-2 replication, and cytopathic effects *in vitro* with doses up to 100 μM showing a survival percentage of 100 % (Fig. 2A). Furthermore, the effect of MG was tested against three variants of concern: B.1.387 (D614G), B.1.429 + B.1.427 (Epsilon), B.1.1.7 (alpha) and B.1.617.2 (delta) showing a significant cell survival after 96 h incubation compared to infected cells with no MG administration (Fig. 2B).

3.2. In vivo effect of metformin glycinate

3.2.1. Demographic and basal characteristics from the clinical study patients

The study included 20 patients (Fig. 3 shows the selection and allocation of the participants) recruited from July 2020 to March 2021, with a follow-up period of 14 days. The mean age was 47.48 (42.83 in group A; 49.38 in group B), 85 % of the patients were male and the average BMI was 28.54 kg/m^2. Table 1 shows the basal parameters and

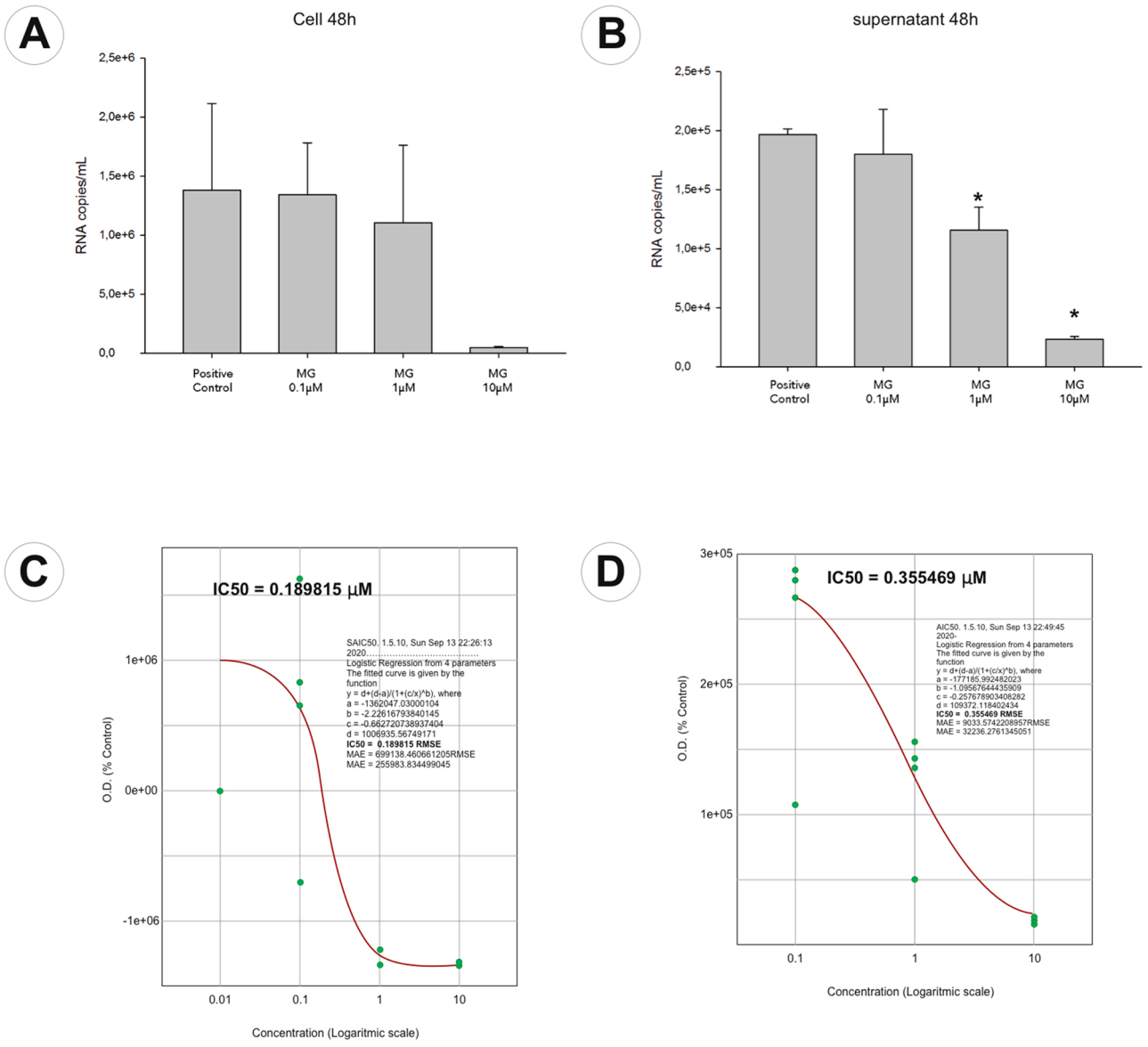

Fig. 1. Metformin glycinate (MG) Inhibition effect on SARS-CoV-2 clinical isolated (MX/BC1/2020). Metformin Glycinate effect on the SARS-CoV-2 (MOI = 100) viral load (RNA copies per mL) determined 48 h after infection in (**A**) supernatant and (**B**) whole cells (carcinoma; non-small cell lung cancer; Cell line H1299). Half-maximal inhibitory concentration (IC50) of MG on cell viability in whole cells (**C**) and supernatant (**D**).

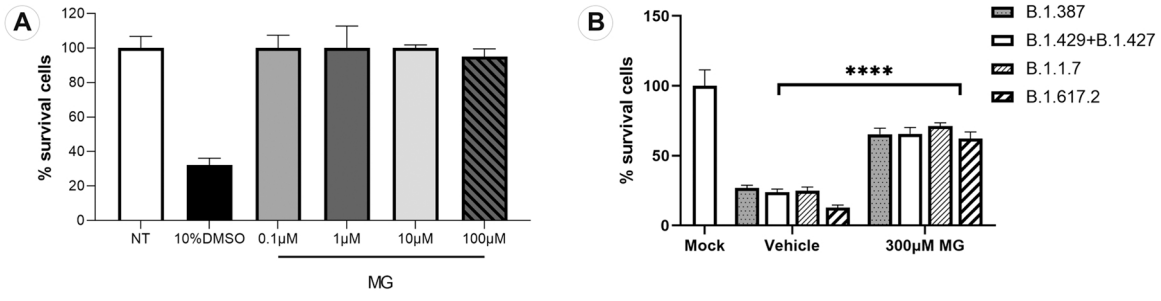

Fig. 2. Evaluation of cytotoxicity of MG in H1299 cells and inhibition of cytopathic effects in Vero E6. (A) Cell viability of H1299 cells after 48 h infection with SARS-CoV-2 clinical isolated (MX/BC1/2020) exposed to different concentration (0.1, 1.0,10 and 100 µM) of MG. 10 % DMSO was used as a dead control, and PBS a negative control (NT). (**B**) Cell viability of Vero E6 cells treated with MG (300 µM) and infected with 0.01pfu/cell of isolated viral strains B.1.387(D614G); B.1.429 +B.1.427 (Epsilon); B.1.1.7 (alpha) or B.1.617.2 (delta).

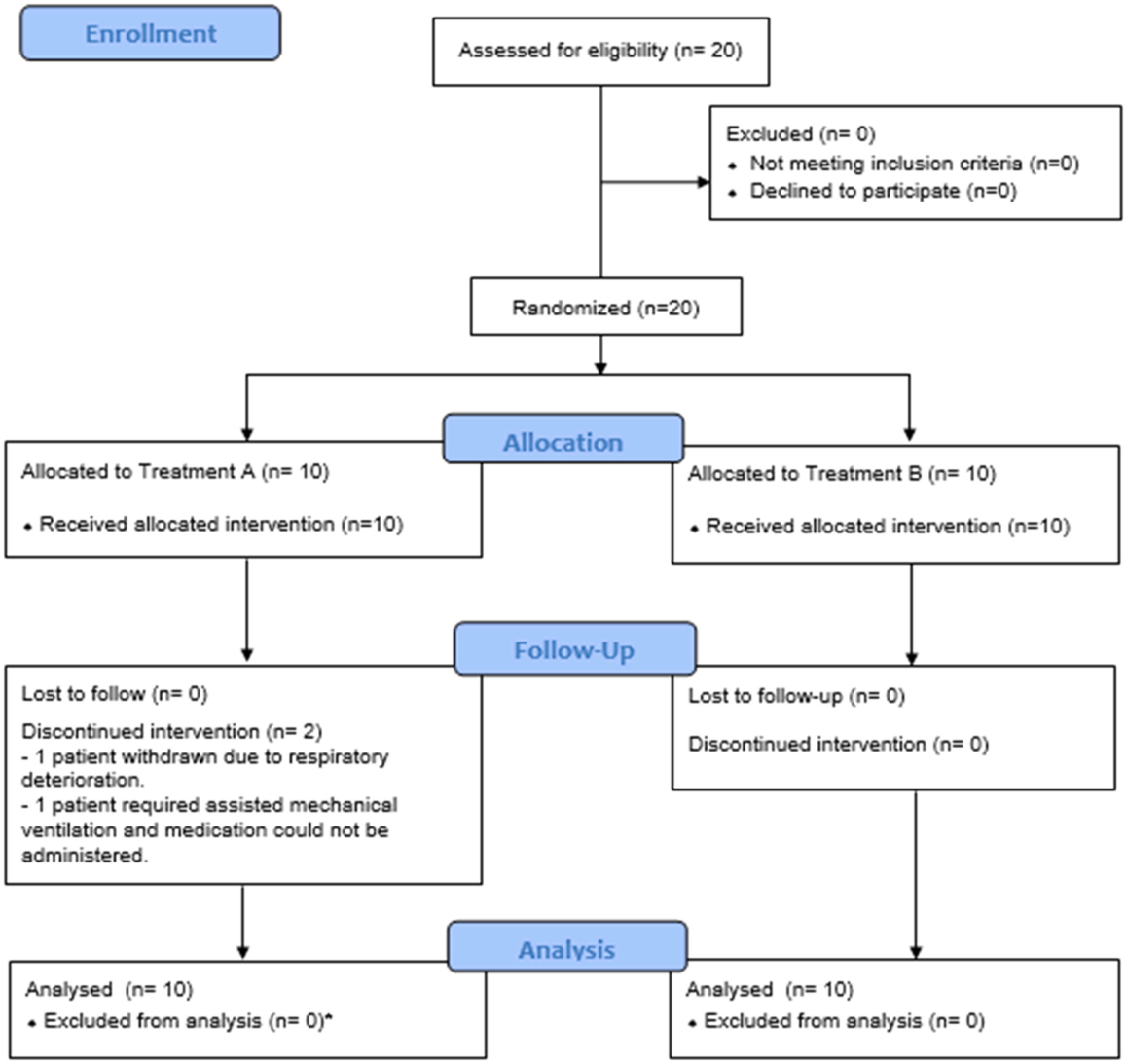

Fig. 3. Flowchart of the selection and allocation of study participants. *No patients were excluded from the statistical analysis since the data obtained was sufficient to be included in the final analysis.

clinical characteristics of the patients. The comorbidities detected were: diabetes 20.0 % (10 % per treatment group), hypertension 20.0 % (group A, 5.0 %; group B, 15.0 %), dyslipidemia 15.0 % (group A, 5.0 %, group B, 10.0 %). There were no important differences between groups, except in the percentage of oxygen saturation, where group B had 93.0 and group A had 89 (the mean percentage was 92.0).

3.2.2. Comparison of the basal main biochemical and immunological parameters between groups of patients from the clinical trial

Table 2 shows the biochemical data for both groups. Essentially, there were no differences between the groups, except in the levels of alkaline phosphatase, where group A had a basal level of 90.5 UI/L and B group had 66.5 UI/L (mean from both groups was 70.5 UI/L), which represents a statistically significant difference ($p = 0.011$).

3.2.3. Basal covid-related symptoms from each group of patients

Table 3 shows that both groups of patients entered the study with similar covid-related symptoms. There were no significant differences in these variables, which included cough, fever, dyspnea, headache, myalgias/arthralgias, diarrhea and a disturbance to the general condition (loss of appetite, fatigue, and weight loss). Additionally, the frequency of other symptoms, such as pharyngitis, tachycardia, abdominal pain, nasal congestion, and abdominal distention, among others, were studied. We did not find significant differences in the basal frequency or percentage of these symptoms between groups.

3.2.4. Comparison of other basal biochemical and immunological parameters between groups of treatment

In addition to analyzing the main biochemical and immunological parameters shown in Table 2, we compared the levels of other variables indicative of inflammation, tissue damage, and severe disease. The results in Table 4 show that both groups of patients entered the study with very similar basal levels of immunoglobulins (IgG and IgM), reactive C protein (RCP), lactate dehydrogenase (DHL), and creatine phosphokinase (CPK).

3.2.5. Comparison of biochemical and immunological parameters in the same group at the beginning and end of the clinical study

There were statistically significant changes in the levels of AST, lymphocytes, neutrophils, D dimer, CRP, DHL, and IgG in the group treated with MG in the beginning and end of the study. In the control group, we observed significant differences at the basal and final state in ALT, ferritin, CRP, and IgG (Table 5).

3.2.6. Evaluation of the need for external oxygen supplementation

Supplementary oxygen requirements were evaluated daily for each

Table 1
Basal demographic and clinical characteristics in each group.

Variable	Treatment A n = 10	Treatment B n = 10	Total n = 20	p
Age (years)	42.83 (32.2; 65.0)	49.38 (45.7; 61.2)	47.48 (39.83; 63.0)	0.247
Sex				
Male (n, %)	8 (40.0)	9 (45.0)	17 (85.0)	1.000
Female (n, %)	2 (10.0)	1 (5.0)	3 (15.0)	
Weight (kg)	84.50 (71.5; 95.0)	85.50 (74.5; 95.0)	84.50 (73.25; 95.0)	0.684
Height (m)	1.72 (1.65; 1.79)	1.75 (1.71–1.77)	1.74 (1.68; 1.78)	0.579
BMI (kg/m^2)	29.1 (22.75; 31.93)	27.72 (25.51; 30.81)	28.54 (24.83; 31.0)	0.684
Clinical characteristics				
SBP (mmHg)	113.0 (109.2; 125.0)	120.0 (118.0; 128.0)	120.0 (112.0; 125.0)	0.165
DBP (mmHg)	70 (65.0; 73.0)	70 (69.0; 78.0)	70.0 (68.0; 76.0)	0.579
CF (lpm)	79 (67.0; 84.0)	70 (66.0; 85.0)	70.0 (67.0; 84.0)	0.684
RF (rpm)	20 (18.0; 20.0)	19 (18.0; 20.0)	20.0 (18.0; 20.0)	0.393
O2 saturation (%)	**89 (88.0; 95.0)**	**93 (90.0; 96.0)**	**92.0 (88.0; 96.0)**	**0.165**
Temperature (°C)	36.5 (36.0; 37.5)	36.2 (36.0; 36.7)	36.4 (36.0; 37.4)	0.529
Comorbidities				
Diabetes (n, %)	2 (10)	2 (10)	4 (20)	1.000
Hypertension (n, %)	1 (5)	3 (15)	4 (20)	0.582
Dyslipidemias (n, %)	1 (5)	2 (10)	3 (15)	1.000
Respiratory disease (n, %)	2 (10)	0 (0)	2 (10)	0.474
Autoimmune disease (n, %)	1 (5)	1 (5)	2 (10)	1.000
Tabaquism (n, %)	1 (5)	1 (5)	2 (10)	1.000

SBP: systolic blood pressure; DBP: diastolic blood pressure; CF: cardiac frequency; RF: respiratory frequency; BMI: body mass index. Medians and interquartile range were used for continuous variables, comparisons between the groups were made through the Mann Whitney U test and for qualitative variables in frequencies and percentages the Fisher's exact-tests were used.

patient during their hospitalization, using the system shown in Table 6. At the end of the study, the points were added and the mean values were compared between groups.

3.2.7. Evaluation of the main efficacy variables between groups

We analyzed three main variables indicative of treatment efficacy: duration of hospitalization, oxygen requirement, and reduction of the percentage of viral load. In the MG-treated group, we observed a significant reduction in the viral load (93.2 %) from the beginning to the end of the study. In the control group, there was only a 78.3 % decrease in the viral load, importantly (Table 7).

Analyzing the number of days necessary to demonstrate an undetectable viral load, it was found that, group A needed only 3.3 days while group B 5.6 days (p = 0.043) (Table 8), the average hospitalization was 8.8 days for group A and 9.8 days for group B, in relation to the need for supplemental oxygen intake, it was found that group A required a lower intake on days 2, 5 and 7 than group B (5.9 *vs* 10.6 points). The differences were statistically significant for all the variables except for the days of hospitalization (Table 7).

It was also determined that patients in group B are 6 times more likely to have a detectable viral load after 4 days (OR = 6.667) compared to group A (Table 8).

Finally, in relation to safety, the number and type of adverse events

Table 2
Basal main biochemical parameters between groups.

Variable	Treatment A	Treatment B	Total	p
Glucose (mg/dL)	151.5 (124.9; 184.3)	148.9 (135.0; 187.7)	148.9 (129.4; 177.3)	0.796
HBA1c (%)	5.95 (5.65; 6.50)	5.8 (4.40; 6.10)	5.8 (5.4; 6.1)	0.529
Total cholesterol (mg/dL)	151.5 (143.0; 189.2)	156.5 (147.2; 173.5)	154.5 (147.0; 176.5)	0.796
HDL cholesterol (mg/dL)	37.5 (26.7; 42.7)	37.5 (32.2; 43.0)	37.0 (29.7; 42.5)	0.529
LDL cholesterol (mg/dL)	91.0 (75.2; 125.2)	102.5 (86.7; 105.2)	97.5 (86.7; 107.2)	0.684
Triglycerides (mg/dL)	169.0 (138.5; 180.0)	137.0 (100.0; 207.5)	157.5 (104.7; 176.5)	0.529
ALT (U/L)	62.5 (30.0; 83.0)	44.0 (30.7; 63.0)	53.0 (30.7; 66.2)	0.436
AST (U/L)	33.8 (23.2; 92.0)	26.4 (21.8; 35.0)	27.6 (22.1; 50.6)	0.089
GGT (U/L)	89.5 (56.7; 112.7)	99.0 (36.0; 134.7)	94.5 (39.2; 129.5)	0.780
Serum creatinine (mg/dl)	0.73 (0.61; 0.81)	0.81 (0.73; 0.93)	0.79 (0.67; 0.87)	0.156
Total bilirubin (mg/dl)	0.29 (0.16; 0.48)	0.37 (0.28; 0.52)	0.31 (0.27; 0.50)	0.315
Albumin (g/L)	3.4 (3.8; 3.8)	3.3 (3.0; 3.4)	3.4 (3.0; 3.6)	0.089
Alkaline phosphatase (UI/L)	**90.5 (71.2; 114.5)**	**66.5 (56.0; 73.2)**	**70.5 (64.2; 91.2)**	**0.011**
Leukocytes (Cell/uL)	12.6 (9.3; 15.0)	10.1 (6.6; 12.9)	10.8 (6.7; 13.6)	0.579
Erythrocytes (Cell/uL)	4.8 (4.3; 5.2)	4.6 (4.2; 5.0)	4.8 (4.2; 5.1)	0.315
Hemoglobin (g/dl)	15.2 (13.5; 15.6)	14.3 (13.4; 15.1)	14.5 (13.5; 15.4)	0.315
Hematocrit (%)	43.4 (40.1; 44.6)	42.6 (39.9; 43.8)	42.9 (40.4; 44.2)	0.247
MCV (fL)	89.6 (84.4; 91.7)	91.6 (87.3; 92.9)	90.4 (87.3; 92.3)	0.247
MCH (pc)	31.2 (29.3; 31.7)	30.9 (29.7; 31.8)	31.0 (29.7; 31.8)	0.684
Platelets (10^9/L)	257.0 (205.2; 339.7)	268.5 (214.5; 307.5)	266.0 (211.7; 307.5)	1.000
Lymphocytes (%)	8.1 (4.0; 11.8)	8.2 (6.7; 11.6)	8.2 (6.0; 11.6)	0.971
Neutrophiles (%)	85.2 (83.4; 89.3)	87.2 (82.5; 89.2)	86.1 (83.2; 89.2)	0.529
Monocytes (%)	4.0 (3.4; 5.7)	3.8 (2.7; 4.4)	3.9 (3.3; 5.0)	0.280

HBA1c: glycated hemoglobin; ALT: alanine aminotransferase; AST: aspartate aminotransferase; GGT: gamma-glutamyl transferase; MCV: mean corpuscular volume; MCH: mean corpuscular hemoglobin. Medians and interquartile range were used for continuous variables, the Mann Whitney U test was for comparisons between treatment groups, qualitative variables frequencies and percentages were used, comparisons were made using the Fisher's exact-tests.

Table 3
Covid-related variables.

Variable	Treatment A n = 10	Treatment B n = 10	Total n = 20	p
Cough (n, %)	8 (40)	7 (35)	15 (75)	1.000
Fever (n, %)	9 (45)	6 (30)	15 (75)	0.303
Dyspnea (n, %)	4 (20)	7 (35)	11 (55)	0.370
Headache (n, %)	7 (35)	3 (15)	10 (50)	0.179
Myalgias/arthralgias (n, %)	6 (30)	6 (30)	12 (60)	1.000
Diarrhea (n, %)	4 (20)	2 (10)	6 (30)	0.628
General condition disturbances (n, %)	5 (25)	7 (35)	12 (60)	0.650

%, percentage. Data presented as frequencies and percentages. Differences between groups were analyzed with the Fisher's exact-tests.

Table 4
Other biochemical and immunological parameters at the beginning of the trial (basal).

Variable	Treatment A n = 10	Treatment B n = 10	Total n = 20	p
D dimer (ng/mL)	533.0 (233.5; 703.5)	480.0 (233.5; 703.5)	511.5 (322.5; 756.5)	0.739
Ferritin (ng/mL)	1335.0 (298.5; 2102.0)	1473.5 (991.2; 2003.0)	1473.5 (754.5; 1987.5)	0.853
Procalcitonin (ng/mL)	0.04 (0.02; 0.13)	0.08 (0.04; 0.22)	0.06 (0.04; 0.17)	0.481
RCP (mg/L)	1.83 (0.47; 2.30)	4.16 (1.47; 11.13)	2.28 (0.74; 7.58)	0.063
DHL (UI/L)	326.5 (255.2; 464.0)	257.5 (237.7; 334.7)	305.5 (241.7; 366.0)	0.105
Interleukin 6 (pg/mL)	13.7 (2.20; 67.35)	8.9 (2.07; 30.62)	10.1 (2.17; 47.0)	0.631
Vitamin D (ng/mL)	19.1 (15.2; 22.8)	23.2 (19.3; 28.0)	20.1 (18.4; 24.3)	0.043
IgG (mg/dl)	1012.0 (753.0; 1106.7)	969.0 (819.0; 1151.7)	1012.0 (819.0; 1116.5)	0.912
IgM (mg/dl)	91.7 (66.4; 119.0)	82.5 (69.0; 115.7)	91.1 (69.1; 115.1)	0.631
CPK (U/L)	41.0 (28.5; 72.7)	35.5 (25.7; 122.7)	39.0 (28.8; 80.5)	0.684

ng/mL, nanograms per milliliter; mg/L, milligrams per liter; IU/L, international units per liter; CRP, C-reactive protein; IgG, immunoglobulin G; IgM, immunoglobulin M; CPK, creatinine phostokinase. Medians and interquartile range were used for continuous variables and comparisons between treatment groups were made with the Mann Whitney U test.

Table 6
Point system for evaluating the need for supplementary oxygen.

Need for supplementary oxygen	Points
1 Not hospitalized	0
2 Hospitalized without oxygen supplementation	1
3 Hospitalized with the requirement of supplementary oxygen (not high flux, non-invasive ventilation).	2
4 Hospitalized with the requirement of non-invasive ventilation and/or high flux oxygen).	4
5 Hospitalized with the requirement of extracorporeal membrane oxygenation and/or invasive mechanical ventilation.	8
6 Death	10

Table 7
Description of the main efficacy variables.

Variable	Treatment A	Treatment B	P*
Days of hospitalization	8.8 ± 6.1	9.8 ± 5.4	0.352
Oxygen need (points)	5.9 ± 4.6	10.6 ± 6.2	0.030
LV% Reduction	93.2 ± 15.4	78.3 ± 62.7	0.013

Expression of results as mean and standard deviation. * Student's t-tests for independent samples were used to compare treatment groups. LV% Percentage viral load.

Table 5
Biochemical and immunological parameters at the beginning and end of the trial.

Variable	Treatment A			Treatment B			
	Basal	Final	p +	Basal	Final	p +	p*
Glucose (mg/dL)	151.5 (124.9; 184.3)	110.3 (78.3;136.2)	.173	148.9 (135.0; 187.7)	139.0 (126.8; 173.4)	.345	.093
Total cholesterol (mg/dL)	151.5 (143.0; 189.2)	160.0 (132.2; 174.5)	.400	156.5 (147.2; 173.5)	185.5 (164.0;203.0)	.069	.142
HDL cholesterol (mg/dL)	37.5 (26.7; 42.7)	35.5 (21.0; 42.7)	.917	37.5 (32.2; 43.0)	51.5 (36.0; 54.2)	.050	.081
LDL cholesterol (mg/dL)	91.0 (75.2; 125.2)	92.5 (74.7; 114.7)	.599	102.5 (86.7; 105.2)	122.5 (46.9; 138.7)	.484	.414
Triglycerides (mg/dL)	169.0 (138.5; 180.0)	147.5 (113.2; 246.0)	.599	137.0 (100.0; 207.5)	114.0 (99.2; 251.25)	.944	.573
ALT (U/L)	62.5 (30.0; 83.0)	85.5 (35.0; 165.2)	.075	**44.0 (30.7; 63.0)**	**92.0 (78.0;110.0)**	**.017**	**.662**
AST (U/L)	**33.8 (23.2; 92.0)**	**31.5 (22.1; 49.7)**	**.028**	26.4 (21.8; 35.0)	22.2 (17.9; 29.8)	.889	.491
GGT (U/L)	89.5 (56.7; 112.7)	84 (33.7; 148.5)	1.000	99.0 (36.0; 134.7)	128.5 (102.7; 175.0)	.262	.142
Serum creatinine (mg/dl)	0.73 (0.61; 0.81)	0.74 (0.60; 0.84)	.600	0.81 (0.73; 0.93)	0.84 (0.72;0.92)	.575	.142
Total bilirubin (mg/dl)	0.29 (0.16; 0.48)	0.35 (0.23; 0.58)	.528	0.37 (0.28; 0.52)	0.47 (0.36; 0.73)	.069	.228
Albumin (g/L)	3.4 (3.8; 3.8)	3.15 (3.07; 3.48)	.345	3.3 (3.0; 3.4)	3.48 (2.95; 3.77)	.440	.662
Alkaline phosphatase (UI/L)	90.5 (71.2; 114.5)	69.0 (56.7; 76.5)	.116	66.5 (56.0; 73.2)	62.0 (59.5; 79.5)	.726	.755
Leukocytes (Cell/uL)	12.6 (9.3; 15.0)	9.4 (6.9; 13.3)	.345	10.1 (6.6; 12.9)	9.9 (6.7; 13.8)	.674	.852
Erythrocytes (Cél/uL)	4.8 (4.3; 5.2)	5.0 (4.17; 7.96)	.345	4.6 (4.2; 5.0)	4.6 (4.4; 4.9)	.441	.282
Hemoglobin (g/dl)	15.2 (13.5; 15.6)	14.8 (12.7; 15.3)	.293	14.3 (13.4; 15.1)	14.5 (13.8; 15.6)	1.000	.852
Hematocrit (%)	43.4 (40.1; 44.6)	43.7 (38.7; 44.8)	.674	42.6 (39.9; 43.8)	41.3 (38.7; 44.7)	.208	.491
MCV (fL)	89.6 (84.4; 91.7)	88.5 (84.8; 91.5)	.345	91.6 (87.3; 92.9)	89.4 (85.4; 92.1)	.208	.573
MCH (pc)	31.2 (29.3; 31.7)	30.8 (27.2; 32.2)	.917	30.9 (29.7; 31.8)	31.3 (29.8; 32.8)	.671	.662
Platelets (10^9/L)	257.0 (205.2; 339.7)	260 (190.7; 346.7)	.916	268.5 (214.5; 307.5)	324.5 (228.5; 441.7)	.208	.491
Lymphocytes (%)	**8.1 (4.0; 11.8)**	**17.0 (5.7; 36.52)**	**.028**	8.2 (6.7; 11.6)	8.0 (5.7; 12.4)	.263	.491
Neutrophiles (%)	**85.2 (83.4; 89.3)**	**76.2 (42.3; 88.7)**	**.046**	87.2 (82.5; 89.2)	85.5 (80.9; 87.8)	.293	.755
Monocytes (%)	4.0 (3.4; 5.7)	7.0 (4.7; 11.0)	.173	3.8 (2.7; 4.4)	3.9 (3.5; 5.8)	.207	.181
D Dimer (ng/mL)	**480.0 (233.5; 703.5)**	**634.0 (171.7; 1315.0)**	**.028**	480.0 (233.5; 703.5)	356.0 (153.5; 1585.09	.237	.491
Ferritin (ng/mL)	1401.5 (360.2; 2523.0)	1289.5 (260.25; 3483.2)	.600	**1709.0 (1199.2; 2179.0)**	**1381.0 (1205.2; 1899.2)**	**.036**	.852
Procalcitonin (ng/mL)	0.08 (0.04; 0.22)	0.04 (0.02;0.21)	.916	0.08 (0.04; 0.22)	0.04 (0.03;0.05)	.018	.755
CRP (mg/L)	**4.16 (1.47; 11.13)**	**0.10 (0.02;0.41)**	**.046**	**4.16 (1.47; 11.13**	**0.09 (0.05; 1.10)**	**.012**	.662
DHL (UI/L)	**257.5 (237.7; 334.7)**	**256.5 (223.7; 295.7)**	**.028**	257.5 (237.7; 334.7)	244.5 (211.0; 296.5)	.208	.852
Interleukin 6 (pg/mL)	8.9 (2.07; 30.62)	2.10 (2.0; 26.2)	.346	8.9 (2.07; 30.62)	2.4 (1.82; 23.8)	.050	.662
Vitamin D (ng/mL)	23.2 (19.3; 28.0)	19.6 (18.5; 31.0)	.249	23.2 (19.3; 28.0)	29.2 (22.1; 36.7)	.484	.345
IgG (mg/dl)	**969.0 (819.0; 1151.7)**	**781.0 (550.0; 873.2)**	**.028**	**969.0 (819.0; 1151.7)**	**800.5 (643.7; 997.7)**	.017	.662
IgM (mg/dl)	82.5 (69.0; 115.7)	220.1 (81.0; 133.99	.116	82.5 (69.0; 115.7)	98.2 (80.9; 147.8)	.327	.573
CPK (U/L)	35.5 (25.7; 122.7)	47.0 (20.7; 76.2)	.833	35.5 (25.7; 122.7)	48.5 (25.7; 76.5)	.674	.950

ng/mL, nanograms per milliliter; mg/L, milligrams per liter; IU/L, international units per liter; CRP, C-reactive protein; IgG, immunoglobulin G; IgM, immunoglobulin M; CPK, creatinine phostokinase. Medians and interquartile range were used for continuous variables * Mann Whitney U test was use to observe differences between treatment groups.

† Wilcoxon test was used for comparisons of changes within groups – 6 cases where no laboratories were performed were excluded from the count.

Table 8
Comparison of negative viral load by treatment group.

Variable	Treatment A n = 10	Treatment B n = 10	P	OR (95 %IC)
Negative viral load (days)	3.3 ± 2.16	5.6 ± 0.89	0.029	
Negative viral load < 3.3 days (n, %)	4.0 (40.0)	0.0 (0.0)	0.043	6.667 (0.596–74.490)
Negative viral load > 4.0 days (n, %)	6.0 (60.0)	10.0 (100.0)		

Expression of results as mean and standard deviation. * For quantitative variables the Student's t-tests for independent samples was used to compare treatment groups. For qualitative variable the Fisher's exact-tests was used for the comparison between treatment groups.

found were similar in both treatment groups, all of them of mild severity. There were no patients with hypoglycemia.

4. Discussion

The potential role of metformin in COVID-19 disease has been elucidated in diverse research highlighting its antioxidant, anti-inflammatory, immunomodulatory, and antiviral effects [22–24]. Our results demonstrate that MG has anti-viral action against the SARS-CoV-2 clinical isolate *in vitro*, with a single dose able to control viral replication within 48 h. SARS–CoV-2 is a positive single-strain RNA virus (+ ssRNA) and depends on cellular membranes in all steps of the viral life cycle and immunologically have similar characteristics concerning host immune response with other +ssRNA viruses, which might offer some insight into the treatment of COVID-19 [25,26]. Plus-stranded RNA viruses share the characteristic of remodeling intracellular membranes in order to create membrane replication factories or replication organelles, which are vesicles where viral RNA replication occurs [27,28]. These vesicles not only represent the site of viral replication but also act as one of the strategies of viral immune evasion mechanisms, shielding the viral RNA from cellular innate immune sensors [29–32]. We hypothesize that MG inhibits the replication of SARS-CoV-2 by the inhibition of protein synthesis as has been described for other RNA viruses. Sphingomyelin (SM) is required for the replication of some RNA viruses as the hepatitis C virus (HCV); the biosynthesis starts in the endoplasmic reticulum (ER) and gives rise to ceramide, which is transported from the ER to the Golgi by the action of ceramide transfer protein (CERT), where it can be converted to a SM. For HCV, it has been demonstrated that inhibition of SM biosynthesis, either by using small-molecule inhibitors or by knockout (KO) of CERT, suppressed HCV replication in a genotype-independent manner. This reduction in HCV replication was rescued by exogenous SM or ectopic expression of the CERT protein, but not by ectopic expression of nonfunctional CERT mutants. Observing low numbers of DMVs in stable replicon cells treated with a SM biosynthesis inhibitor or in CERT-KO cells transfected with either HCV replicon or with constructs that drive HCV protein production in a replication-independent system indicated the significant importance of SM to DMVs. The degradation of SM of the *in vitro*-isolated DMVs affected their morphology and increased the vulnerability of HCV RNA and proteins to RNase and protease treatment, respectively [33,34].

The SARS-CoV-2 can induce cell death after 48–72 h of infection; therefore, the cell viability is a surrogate measure of viral replication *in vitro*. Pre-treatment of cells with a single-dose of 300 μM MG was able to reduce cell death among different SARS-CoV2 variants, indicating that MG cellular mechanism is kept despite differences in SARS-CoV2 spike.

The *in vitro* results are in line with our clinical study where we demonstrated that MG reduces the viral load of Covid-19 patients to undetectable levels in only 3.3 days. This reduction of infection is associated with shorter hospitalization and less dependence on supplementary oxygen. Except for a mildly elevated GGT in both groups, in the basal and final state, most of the biochemical parameters evaluated at the beginning and end of the clinical study were normal for the MG and control group. The only two-biochemical markers that changed significantly with MG treatment were AST and LDH levels. AST levels were significantly reduced at the end of the study in the group treated with MG (33.8–31.5 U/L, basal *vs* final, respectively), but both levels are in the normal range (8–48 U/L). Similarly, LDH levels decreased in the MG group from 257.5 to 256.5 IU/L, both of which are within the normal range for this enzyme. D dimer was above the normal range in both groups at the beginning of the study (480.0 ng/mL for both groups), as can be expected for Covid-19 patients [35]. Interestingly, D dimer increased significantly only in the MG group at the end of the treatment (480.0–634.0 ng/mL), while a non-significant decrease was observed for the control group (480.0–356.0 ng/mL).

Even though the majority of patients from both groups entered the study with moderate disease, we did not observe the expected elevated C reactive protein level for Covid patients (20–50 mg/L) [36]. In fact, both groups had normal CRP levels at the beginning (4.16 mg/L, both groups) and these levels decreased significantly in all patients at the end of the study (0.10 and 0.09 mg/L, MG and control groups, respectively). This could be explained by the fact that none of the patients that entered this study presented with severe Covid symptoms. Basal fasting glucose levels were elevated in both groups (151.5 and 148.9 mg/dL, respectively). This is not surprising, as 50 % of hospitalized Covid patients develop acute hyperglycemia, and 7 % of this population has diabetes [37]. At the end of the study, glucose levels in the MG-treated group were close to normal (110.3 mg/dL), as was expected from the anti-hyperglycemic mode of action of the drug.

5. Conclusions

In the present study, we demonstrated the *in vitro* effect of metformin glycinate on the viral load of SARS-CoV-2. The antiviral effect of MG was supported by *in vivo* results according to biochemical and immunological parameters; 620 mg of MG administered orally every 12 h significantly and safely decreased viral load in Covid 19 patients. Although these results strongly suggest that MG could be repositioned for the treatment of SARS-CoV2, further clinical studies need to be assessed to establish the safety and efficacy of MG in large populations. The hospitalization condition of the patients was one of the limitations of the clinical study, which made the collection of complete data and follow-up of subjects more complicated. A longer follow-up could elucidate if the biochemical alterations found in this study (reduced AST and reduced DHL) are clinically relevant or are the only biochemical modifications. Finally, the longer follow-up could determine if the ability to decrease viral replication of MG would have an implication on subacute and/or chronic complications of the COVID-19 patients.

CRediT authorship contribution statement

Claudia Ventura-Lopez: Formal analysis, Investigation, Methodology Writing – original draft. **Karla Cervantes-Luevano:** Formal analysis, Data curation, Methodology. **Janet S. Aguirre-Sánchez:** Formal analysis, Data curation, Methodology. **Juan C. Flores-Caballero:** Formal analysis, Methodology. **Carolina Alvarez-Delgado:** Data curation, Writing – original draft. **Johanna Bernaldez-Sarabia:** Supervision, Project administration. **Noemí Sánchez-Campos:** Data curation. **Laura A. Lugo-Sánchez:** Methodology, Writing – review & editing. **Ileana C. Rodríguez-Vázquez:** Methodology, Writing – review & editing. **Jose G. Sander-Padilla:** Methodology, Writing – review & editing. **Yulia Romero-Antonio:** Methodology, Writing – review & editing. **María M. Arguedas-Núñez:** Methodology, Writing – review & editing. **Jorge González-Canudas:** Conceptualization, Resources, Supervision, Writing – review & editing. **Alexei F. Licea-Navarro:** Funding acquisition, Project administration, Supervision, Writing – review &

editing.

Funding

Funding for this work came partially from CICESE Grant 685-101.

Declaration of Competing Interest

The authors declare that they have no known competing financial interests or personal relationships that could have appeared to influence the work reported in this paper.

Data availability

Data will be made available on request.

Acknowledgments

We are grateful to Dr. Javier Perez-Robles, Dr. Jahaziel Gasperin and M.A. Itandehui Betanzo Gutiérrez for support during samples processing.

References

[1] World Health Organization, Coronavirus disease situation, 2022. ⟨https://covid19.who.int/⟩, (Accessed 27 April 2022).
[2] T.S. Fung, D.X. Liu, Human coronavirus: host-pathogen interaction, Annu. Rev. Microbiol. 73 (2019) 529–557, https://doi.org/10.1146/annurev-micro-020518-115759.
[3] R.J. Ford, M.D. Fullerton, S.L. Pinkosky, E.A. Day, J.W. Scott, J.S. Oakhill, A. L. Bujak, B.K. Smith, J.D. Crane, R.M. Blümer, K. Marcinko, B.E. Kemp, H. C. Gerstein, G.R. Steinberg, Metformin and salicylate synergistically activate liver AMPK, inhibit lipogenesis and improve insulin sensitivity, Biochem. J. 468 (2015) 125–132, https://doi.org/10.1042/BJ20150125.
[4] National Library of Medicine (U.S.), Metformin Glycinate on Metabolic Control and Inflammatory Mediators in Type 2 Diabetes (COMET), Identifier NCT01386671, 2018. Available from: ⟨https://clinicaltrials.gov/ct2/show/study/NCT01386671⟩.
[5] J. González-Canudas, Comet Group, 146-LB: efficacy and safety of metformin glycinate vs. metformin hydrochloride in metabolic control and inflammatory mediators in Type 2 diabetes mellitus patients (T2DM), ADA (2019) 68, https://doi.org/10.2337/db19-146-LB.
[6] P. Rada, A. Mosquera, J. Mutané, F. Ferrandiz, L. Rodríguez-Mañas, F. de Pablo, J. González-Canudas, A.M. Malverde, Differential effects of metformin glycinate and hydrochloride in glucose production, AMPK phosphorylation and insulin sensitivity in hepatocytes from non-diabetic and diabetic mice, Food Chem. Toxicol. 123 (2019) 470–480, https://doi.org/10.1016/j.fct.2018.11.019.
[7] D.G. Hardie, F.A. Ross, S.A. Hawley, AMPK: a nutrient and energy sensor that maintains energy homeostasis, Nat. Rev. Mol. Cell Biol. 13 (2012) 251–262, https://doi.org/10.1038/nrm3311.
[8] L.J. Foster, M.L. Weir, D.Y. Lim, Z. Liu, W.S. Trimble, A. Klip, A functional role for VAP-33 in insulin-stimulated GLUT4 traffic, Traffic 1 (2000) 512–521, https://doi.org/10.1034/j.1600-0854.2000.010609.x.
[9] L. Florin, A. Pegel, E. Becker, A. Hausser, M.A. Olayioye, H. Kaufmann, Heterologous expression of the lipid transfer protein CERT increases therapeutic protein productivity of mammalian cells, J. Biotechnol. 141 (2009) 84–90, https://doi.org/10.1016/j.jbiotec.2009.02.014.
[10] A. Raya, F. Revert-Ros, P. Martinez-Martinez, S. Navarro, E. Rosello, B. Vieites, F. Granero, J. Forteza, J. Saus, Goodpasture antigen-binding protein, the kinase that phosphorylates the goodpasture antigen, is an alternatively spliced variant implicated in autoimmune pathogenesis, J. Biol. Chem. 275 (2000) 40392–40399, https://doi.org/10.1074/jbc.M002769200.
[11] M. Kawano, K. Kumagai, M. Nishijima, K. Hanada, Efficient trafficking of ceramide from the endoplasmic reticulum to the Golgi apparatus requires a VAMP-associated protein-interacting FFAT motif of CERT, J. Biol. Chem. 281 (2006) 30279–30288, https://doi.org/10.1074/jbc.M605032200.
[12] S. Saito, H. Matsui, M. Kawano, K. Kumagai, N. Tomishige, K. Hanada, S. Echigo, S. Tamura, T. Kobayashi, Protein phosphatase 2Cepsilon is an endoplasmic reticulum integral membrane protein that dephosphorylates the ceramide transport protein CERT to enhance its association with organelle membranes, J. Biol. Chem. 283 (2008) 6584–6593, https://doi.org/10.1074/jbc.M707691200.
[13] D.C. Prosser, D. Tran, P.Y. Gougeon, C. Verly, J.K. Ngsee, FFAT rescues VAPA-mediated inhibition of ER-to-Golgi transport and VAPB-mediated ER aggregation, J. Cell Sci. 121 (2008) 3052–3061, https://doi.org/10.1242/jcs.028696.
[14] Y. Zhang, Y. Wang, C. Bao, Y. Xu, H. Shen, J. Chen, J. Yan, Y. Chen, Metformin interacts with AMPK through binding to gamma subunit, Mol. Cell. Biochem. 368 (2012) 69–76, https://doi.org/10.1007/s11010-012-1344-5.
[15] F.J. Díaz, W. Aguilar-Jiménez, L. Flórez-Álvarez, G. Valencia, K. Laiton-Donato, C. Franco-Muñoz, D. Álvarez-Díaz, M. Mercado-Reyes, M.T. Rugeles, Isolation and characterization of an early SARS-CoV-2 isolate from the 2020 epidemic in Medellín, Colombia. Aislamiento y caracterización de una cepa temprana de SARS-CoV-2 durante la epidemia de 2020 en Medellín, Colombia, Biomed.: Rev. Inst. Nac. Salud 40 (2020) 148–158, https://doi.org/10.7705/biomedica.5834.
[16] L.J. Reed, H. Muench, A simple method of estimating fifty per cent endpoints, Am. J. Epidemiol. 27 (1983) 493–497, https://doi.org/10.1093/oxfordjournals.aje.a118408.
[17] L.A. Sachs, D. Schnurr, S. Yagi, M.E. Lachowicz-Scroggins, J.H. Widdicombe, Quantitative real-time PCR for rhinovirus, and its use in determining the relationship between TCID50 and the number of viral particles, J. Virol. Methods 171 (2011) 212–218, https://doi.org/10.1016/j.jviromet.2010.10.027.
[18] M.A. Ramakrishnan, Determination of 50 % endpoint titer using a simple formula, World J. Virol. 5 (2016) 85–86, https://doi.org/10.5501/wjv.v5.i2.85.
[19] V.M. Corman, O. Landt, M. Kaiser, R. Molenkamp, A. Meijer, D.K. Chu, T. Bleicker, S. Brünink, J. Schneider, M.L. Schmidt, D.G. Mulders, B.L. Haagmans, B. Van der Veer, S. Van den Brink, L. Wijsman, G. Goderski, J.L. Romette, J. Ellis, M. Zambon, M. Peiris, H. Goossens, C. Reusken, M.P. Koopmans, C. Drosten, Detection of 2019 novel coronavirus (2019-nCoV) by real-time RT-PCR, Eur. Surveill. 25 (2020), 2000045, https://doi.org/10.2807/1560-7917.ES.2020.25.3.2000045 (Erratum in: Euro Surveill. 2020 Apr;25(14): Erratum in: Euro Surveill. 2020 Jul;25(30): Erratum in: Euro Surveill. 2021 Feb;26(5)).
[20] A.H. Cory, T.C. Owen, J.A. Barltrop, J.G. Cory, Use of an aqueous soluble tetrazolium/formazan assay for cell growth assays in culture, Cancer Commun. 3 (1991) 207–212, https://doi.org/10.3727/095535491820873191.
[21] T.L. Riss, R.A. Moravec, Comparison of MTT, XTT, and a novel tetrazolium compound for MTS for *in vitro* proliferation and chemosensitivity assays, Mol. Biol. Cell 3 (Suppl.) (1992) S184a.
[22] L. Ojeda-Fernández, A. Foresta, G. Macaluso, P. Colacioppo, M. Tettamanti, A. Zambon, S. Genovese, I. Fortino, O. Leoni, M.C. Roncaglioni, M. Baviera, Metformin use is associated with a decrease in the risk of hospitalization and mortality in COVID-19 patients with diabetes: a population-based study in Lombardy, Diabetes Obes. Metab. 24 (5) (2022) 891–898, https://doi.org/10.1111/dom.14648.
[23] S.M. Samuel, E. Varghese, D. Büsselberg, Therapeutic potential of metformin in COVID-19: reasoning for its protective role, Trends Microbiol. 29 (10) (2021) 894–907, https://doi.org/10.1016/j.tim.2021.03.004.
[24] E. Varghese, S.M. Samuel, A. Liskova, P. Kubatka, D. Büsselberg, Diabetes and coronavirus (SARS-CoV-2): molecular mechanism of metformin intervention and the scientific basis of drug repurposing, PLoS Pathog. 17 (6) (2021), e1009634, https://doi.org/10.1371/journal.ppat.1009634.
[25] N. Altan-Bonnet, Lipid tales of viral replication and transmission, Trends Cell Biol. 27 (2017) 201–213, https://doi.org/10.1016/j.tcb.2016.09.011.
[26] H. Alothaid, M. Aldughaim, K. El Bakkouri, S. AlMashhadi, A.A. Al-Qahtani, Similarities between the effect of SARS-CoV-2 and HCV on the cellular level, and the possible role of ion channels in COVID19 progression: a review of potential targets for diagnosis and treatment, Channels 14 (2020) 403–412, https://doi.org/10.1080/19336950.2020.1837439.
[27] D. Egger, B. Wolk, R. Gosert, L. Bianchi, H.E. Blum, D. Moradpour, K. Bienz, Expression of hepatitis C virus proteins induces distinct membrane alterations including a candidate viral replication complex, J. Virol. 76 (2002) 5974–5984, https://doi.org/10.1128/jvi.76.12.5974-5984.2002.
[28] H. Wang, A.W. Tai, Mechanisms of cellular membrane reorganization to support hepatitis C virus replication, Viruses 8 (2016) 142, https://doi.org/10.3390/v8050142.
[29] M. Kikkert, Innate immune evasion by human respiratory RNA viruses, J. Innate Immun. 12 (2020) 4–20, https://doi.org/10.1159/000503030.
[30] I. Romero-Brey, R. Bartenschlager, Membranous replication factories induced by plus-strand RNA viruses, Viruses 6 (2014) 2826–2857, https://doi.org/10.3390/v6072826.
[31] A. Garcia-Sastre, Ten strategies of interferon evasion by viruses, Cell Host Microbe 22 (2017) 176–184, https://doi.org/10.1016/j.chom.2017.07.012.
[32] Y.T. Kao, M.M.C. Lai, C.Y. Yu, How dengue virus circumvents innate immunity, Front. Immunol. 7 (2018) 2860, https://doi.org/10.3389/fimmu.2018.02860.
[33] Y. Amako, G.H. Syed, A. Siddiqui, Protein kinase D negatively regulates hepatitis C virus secretion through phosphorylation of oxysterol-binding protein and ceramide transfer protein, J. Biol. Chem. 286 (2011) 11265–11274, https://doi.org/10.1074/jbc.M110.182097.
[34] H. Gewaid, H. Aoyagi, M. Arita, K. Watashi, R. Suzuki, S. Sakai, K. Kumagai, T. Yamaji, M. Fukasawa, F. Kato, T. Hishiki, A. Mimata, Y. Sakamaki, S. Ichinose, K. Hanada, M. Muramatsu, T. Wakita, H. Aizaki, Sphingomyelin is essential for the structure and function of the double-membrane vesicles in hepatitis C virus RNA replication factories, J. Virol. 94 (2020), https://doi.org/10.1128/JVI.01080-20 (e01080 – 20).
[35] Y. Yao, J. Cao, Q. Wang, Q. Shi, K. Liu, Z. Luo, X. Chen, S. Chen, K. Yu, Z. Hang, D-dimer as a biomarker for disease severity and mortality in COVID-19 patients: a case control study, J. Intensive Care 8 (2020) 49, https://doi.org/10.1186/s40560-020-00466-z.
[36] N. Ali, Elevated level of C-reactive protein may be an early marker to predict risk for severity of COVID-19, J. Med. Virol. 92 (2020) 2409–2411, https://doi.org/10.1002/jmv.26097.
[37] A. Ceriello, Hyperglycemia and COVID-19: what was known and what is really new? Diabetes Res. Clin. Pract. 167 (2020), 108383 https://doi.org/10.1016/j.diabres.2020.108383.